Biochimica et Biophysica Acta 1787 (2009) 393–401

Contents lists available at ScienceDirect

Biochimica et Biophysica Acta

journal homepage: www.elsevier.com/locate/bbabio

IF1, the endogenous regulator of the F_1F_o-ATPsynthase, defines mitochondrial volume fraction in HeLa cells by regulating autophagy

Michelangelo Campanella [a,c,*,1], Andreas Seraphim [a], Rosella Abeti [a], Edward Casswell [a], Pedro Echave [b], Michael R. Duchen [a]

[a] Department of Cell and Developmental Biology, Mitochondrial Biology Group, University College London, UK
[b] Wolfson Institute for Biomedical Research, University College London, UK
[c] Royal Veterinary College University of London, UK

ARTICLE INFO

Article history:
Received 31 December 2008
Received in revised form 23 February 2009
Accepted 24 February 2009
Available online 5 March 2009

Keywords:
IF1
Mitochondria
Autophagy
ROS
F_1F_o-ATPsynthase

ABSTRACT

The protein IF1 limits mitochondrial ATP consumption when mitochondrial respiration is impaired by inhibiting the 'reverse' activity of the F_1F_o-ATPsynthase. We have found that IF1 also increases F_1F_o-ATPsynthase activity in respiring mitochondria, promoting its dimerization and increasing the density of mitochondrial cristae. We also noted that IF1 overexpression was associated with an increase in mitochondrial volume fraction that was conversely reduced when IF1 was knocked down using small interfering RNA (siRNA). The volume change did not correlate with the level of transcription factors involved in mitochondrial biogenesis. However, autophagy was dramatically increased in the IF1siRNA treated cells (−IF1), assessed by quantifying LC3-GFP translocation to autophagosomes, whilst levels of autophagy were low in IF1 overexpressing cells (+IF1). The increase in LC3-GFP labelled autophagosomes in −IF1 cells was prevented by the superoxide dismutase mimetic, manganese (III) tetrakis (4-benzoic acid) porphyrin (MnTBAP). An increase in the basal rate of generation of reactive oxygen species (ROS) in −IF1 cells was demonstrated using the fluorescent probe dihydroethidium (DHE). Thus, IF1 appears to limit mitochondrial ROS generation, limiting autophagy which is increased by IF1 knockdown. Variations in IF1 expression level may therefore play a significant role in defining both resting rates of ROS generation and cellular mitochondrial content.

1. Introduction

Mitochondria produce the majority of ATP required for cellular processes, shape $[Ca^{2+}]_c$ signalling and play an active role in cell death. The F_1F_o-ATPsynthase, a transmembrane molecular motor driven by the electrochemical potential ($\Delta\psi_m$) established across the inner mitochondrial membrane by respiration [1–4], plays a central role in cellular energy homeostasis. As a proton motive ATPase, its equilibrium is determined by the balance of energy provided by the phosphorylation potential on one hand and by $\Delta\psi_m$ on the other [5]. Following inhibition of respiration, the potential will reach a new equilibrium where the enzyme may reverse, pumping protons across the inner mitochondrial membrane and so consuming ATP to maintain $\Delta\psi_m$. The inhibitor factor 1 (IF1), a nuclear encoded protein of 84 amino acids, limits this activity (for review see [6]). We have recently explored the consequences of altered IF1 expression levels and found that the inhibitory efficacy of IF1 on the mitochondrial F_1F_0-ATPase in response to inhibition of mitochondrial respiration was increased by IF1 overexpression, whilst IF1 suppression permits reversal of the mitochondrial F_1F_o-ATPase and consequent ATP consumption [7]. We also found that IF1 influences mitochondrial structure and function such that IF1 overexpression increased cristae formation and seemed to increase proton flux through the synthase. This was accompanied by a more oxidised NADH:NAD^+ ratio. Suppression of IF1 expression had opposite effects: a decrease in the number of mitochondrial cristae and a reduction of H^+ flux through the F_1F_o-ATPsynthase and consequent a more reduced state of the NADH:NAD^+ ratio [7]. In the course of these experiments we noted that mitochondria were relatively sparse in cells in which IF1 was knocked down and enriched in cells with overexpression of IF1. The present paper describes our efforts to identify the mechanisms underlying these observations, which prove to result not from changes in mitochondrial biogenesis, but rather from modulation of the autophagy pathways that are upregulated in cells in which IF1 is suppressed.

Autophagy is the only process by which organelles of a dimension of mitochondrion can be sequestered and subsequently delivered to lysosomes for hydrolytic digestion [8]. During autophagy, an isolation

* Corresponding author. Department of Cell and Developmental Biology, Mitochondrial Biology Group, University College London, UK.
E-mail addresses: mcampanella@rvc.ac.uk (M. Campanella), m.duchen@ucl.ac.uk (M.R. Duchen).
[1] Current address: Department of Veterinary Basic Science, Royal Veterinary College, University of London, UK.

0005-2728/$ – see front matter © 2009 Elsevier B.V. All rights reserved.
doi:10.1016/j.bbabio.2009.02.023

membrane forms a cupshaped structure called pre-autophagosome that eventually envelops the autophagic target becoming an autophagosome. The latter fuses with lysosomes to form autolysosomes within their sequestered contents are degraded by lysosoal hydrolyses and recycled [9–12] A machinery of genetically conserved autophagy-related proteins was first identified in yeast under a complex of Atg proteins [13]. These Atg proteins include: (i) Atg1, Atg13, and Atg17, serine–threonine kinase complex involved in autophagic induction; (ii) a class II phosphatydilcholine-3-kinase (PI3K) complex which functions in vesicle nucleation; (iii) Atg12 and atg8, ubiquitin-like protein conjugating systems, involved in vesicle extension and completion together with Atg5, Atg7, Atg10 and Atg16 [14]. In mammalian cells, activation of autophagy is controlled by two classes of PI3Ks with opposite effects, Target of Rapamycin (mTOR) that blocks autophagy [15] and class III PI3Ks that stimulates it [16]. Selectivity of autophagy toward intracellular organelles was demonstrated in the past for the peroxisomes [17] and there is now a general consensus that damaged mitochondria can also be eliminated in a process of organelle selective autophagy, termed mitophagy. The regulatory mechanisms as well as the molecules dictating the onset of this process remain ill-defined. Here we provide evidence suggesting that IF1 may play a significant role in this process of mitochondria selection – quality control – so defining the overall dimension of the mitochondrial network in HeLa cells.

2. Results

2.1. IF1 expression level affects mitochondrial morphology

HeLa cells were transfected with mitochondrially targeted GFP either alone or together with IF1 or a siRNA for IF1. Cells were also loaded with calcein blue to identify the margins and dimensions of the cell. Mitochondrial volume fraction was then calculated as a fraction of the total cell volume (see Materials and methods). The fractional volume occupied by mitochondria clearly varied with IF1 expression level, increasing from a control value of 28.4% ± 5.4 to 44.6% ± 10.3 in IF1 overexpressing cells, which showed a denser, more widely distributed mitochondrial network. Cells treated with siRNA against IF1 consistently showed a more fragmented network with a significant reduction in the mitochondrial volume fraction to 20.1% ± 5.3(Fig. 1) compared to control cells (**$p<0.01$, *$p<0.05$, $n=3$ sets of transfection per type).

2.2. Changes in IF1 expression do not alter the expression of proteins responsible for mitochondrial biogenesis

IF1 induced changes in mitochondrial volume fraction might result from changes in the expression of the major transcription factors involved in the coordination of mitochondrial biogenesis — peroxisome proliferator-activated receptor-γ coactivator (PGC-1) [18] peroxisome proliferator-activated receptor γ coactivator-related 1 (*PPRC1*) [19] *and* transcription factor A of the mitochondria, (TFAM) [20]. We therefore used quantitative rtPCR (RT-QPCR) to explore the expression of these genes in cells with overexpression or suppression of IF1. The mRNA analysis (Fig. 2A) did not show any significant increase, but rather a statistically significant decrease in mRNA for both PGC-1 and PPRC1 (PGC1, control: 1.095 ± 0.13, +IF1:0.57 ± 0.26, arbitrary units, A.U. *$p<0.05$; PPRC1, control: 0.95 ± 0.058, +IF1: 0.56 ± 0.10, fluorescence units *$p<0.05$, $n=3$ sets of transfection) whilst TFAM remained unchanged (Control: 1.044 ± 0.05; +IF1: 0.93 ± 0.07, A.U., $n=3$ sets of transfection). This finding led us to consider other potential mechanisms that might regulate mitochondrial volume. Since autophagy is the only known mechanism that selectively removes organelles for degradation, we explored its possible role in defining mitochondrial volume in these cells.

2.3. IF1 sets low basal levels of autophagy by regulating mitochondrial ROS generation

In order to explore whether alterations in IF1 level of expression modulates the levels of autophagy in HeLa cells we followed the distribution of the fusion protein LC3-GFP after transient co-transfection with IF1 or the siRNA against IF1. During activation of autophagy pathways, 22 amino acids are cleaved from the C-terminus of LC3, forming LC3-II that is lipidated and selectively localized to newly formed autophagosomes. Hence, we used LC3-GFP distribution within the cell to quantify the degree of basal autophagy in relation to IF1 expression. This was quantified by measuring the standard deviation of the signal across the cell as a function of the mean signal intensity — a measure of the localization of the signal (for methods see [21]). Fig. 2 panel Bi shows that control and +IF1 cells have a minimal number of autophagosomes since in both cases LC3-GFP is uniformly distributed throughout the cytosol with a minimally punctuate signal. However, the −IF1 cells showed a significant increase in the compartmentalization of the marker, consistent with a model involving the translocation of LC3-GFP from the cytosol into the membranes of newly formed autophagosomes, creating a punctate pattern.

Quantification of LC3-GFP translocation (Fig. 2Bii) showed that the average SD/mean ratio was statistically significantly different in both +IF1 and −IF1 compared to control cells (Control: 0.49 ± 0.02, $n=173$; +IF1: 0.42 ± 0.01, $n=152$; −IF1: 0.64 ± 0.03, $n=185$ *$p<0.05$, **$p<0.01$). In −IF1 cells, the increase in SD/mean ratio, resulting from the increase in variability of pixel intensity, confirms a greater level of not induced autophagic activity in these cells. Conversely, the average SD/mean ratio of +IF1 cells was reduced compared to controls suggesting a reduced autophagic activity.

Thus, it seems that basal autophagic activity varies according to the expression levels of IF1 in HeLa cells. We therefore explored possible pathways by which IF1 might mediate such an effect. An increase in the generation of reactive oxygen species (ROS) can activate the autophagy pathway [22–24]. As the mitochondria in −IF1 cells have a more reduced NADH:NAD+ ratio and a bigger membrane potential, both conditions that tend to increase mitochondrial ROS generation, this seemed a plausible mechanism. We therefore tested whether MnTBAP, a membrane permeant SOD mimetic and ROS scavenger [25] might influence the development of autophagy. Therefore, 24 h after transfection with siRNA for IF1 cells were treated with 5 μM MnTBAP for 12 h before confocal imaging and analysis. In cells treated with MnTBAP, the differences in SD/mean ratios of the LC3-GFP signal between the three cohorts of cells were effectively removed (Control: 0.41 ± 0.016, $n=170$ +IF1: 0.41 ± 0.019, $n=102$; −IF1: 0.40 ± 0.010, $n=114$ *$p<0.05$). IF1 overexpression failed to alter autophagosome formation triggered by treatment of cells with Hydrogen peroxide H_2O_2 (10^{-6}M, 2 h) or Rapamycin (5 μM, 4 h) (Fig. 2C). Also in this case the SD/mean ratios of LC3-GFP distribution between control and +IF1 cells was calculated to evaluate the degree of autophagic activity that did not show any statistically significant difference between the two (H_2O_2, Control: 0.64 ± 0.10; +IF1: 0.57 ± 0.086 $n=73$ per cell type; Rapamycin, Control: 0.66 ± 0.09; +IF1: 0.60 ± 0.13; $n=35$ per cell type, SD/mean ratios, $p>0.05$). This indicates that IF1 modulates autophagic activity through an intrinsic mechanism but does not influence downstream pathways in the activation of this pathway.

2.4. Reactive oxygen species (ROS) generation is increased in −IF1 cells and underlies the decreased mitochondrial volume

The above data suggest that ROS generation might be increased in the siRNA treated cells in which IF1 expression is suppressed. We therefore measured the rate of ROS production in cells expressing different levels of IF1 using the fluorescent probe Dihydroethidium (DHE, 10 μM), which is oxidised to a fluorescent product by ROS, so that

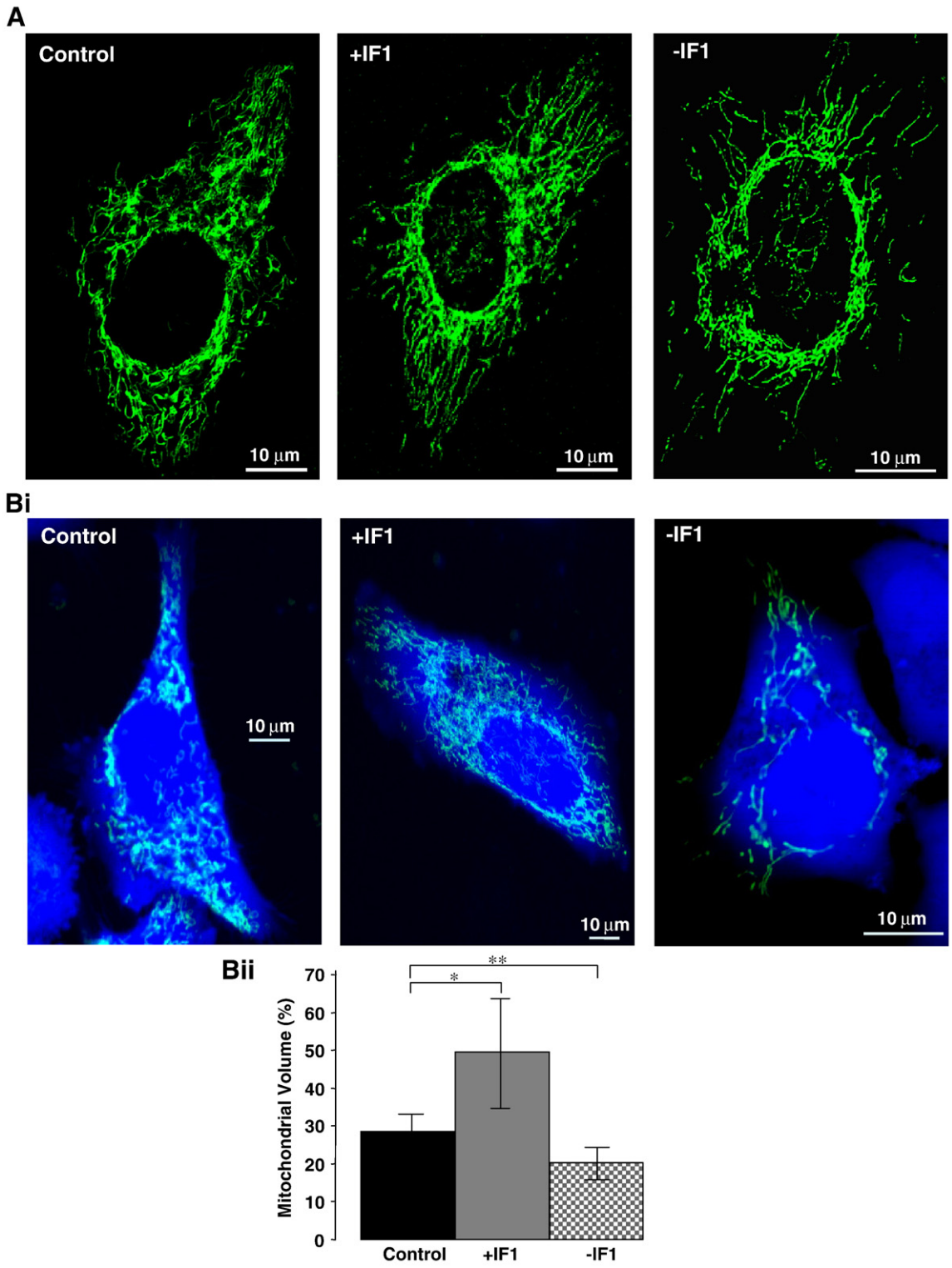

Fig. 1. IF1 level of expression causes alterations in the mitochondrial volume fraction. (A) Projections of confocal Z-stacks of HeLa cells expressing mitochondrially targeted GFP and different levels of IF1 expression. IF1 overexpressing cells (+IF1) showed an increased density of the mitochondrial network compared to control cells and those treated with siRNA for IF1 (−IF1) which, on the contrary, showed a significant decrease in the density of the mitochondrial network. (Bi) By staining the cytosol with calcein blue, the % of cellular volume occupied by mtGFP was quantified as shown in panel Bii.

the rate of fluorescence increase is a function of the rate of ROS generation [26–30]. The traces shown in Fig. 3A, show that in −IF1 cells, DHE was oxidised at a significantly higher rate than in control and +IF1 cells [Control: $(4.7 \pm 1.7) \cdot 10^{-4}$; +IF1: $(4.9 \pm 1.0) \cdot 10^{-4}$; −IF1: $9.3 \cdot 10^{-4} \pm 7.5 \cdot 10^{-5}$ Δfluorescence units/Δseconds, $^{**}p<0.001$; $n=23$ per cell type out of 5 sets of transfection]. These data together show that ROS generation is increased in cells in which IF1 expression is suppressed, consistent with the suggestion that autophagy and a reduction in mitochondrial volume fraction are triggered by increased ROS generation. We therefore asked whether the ROS scavenger

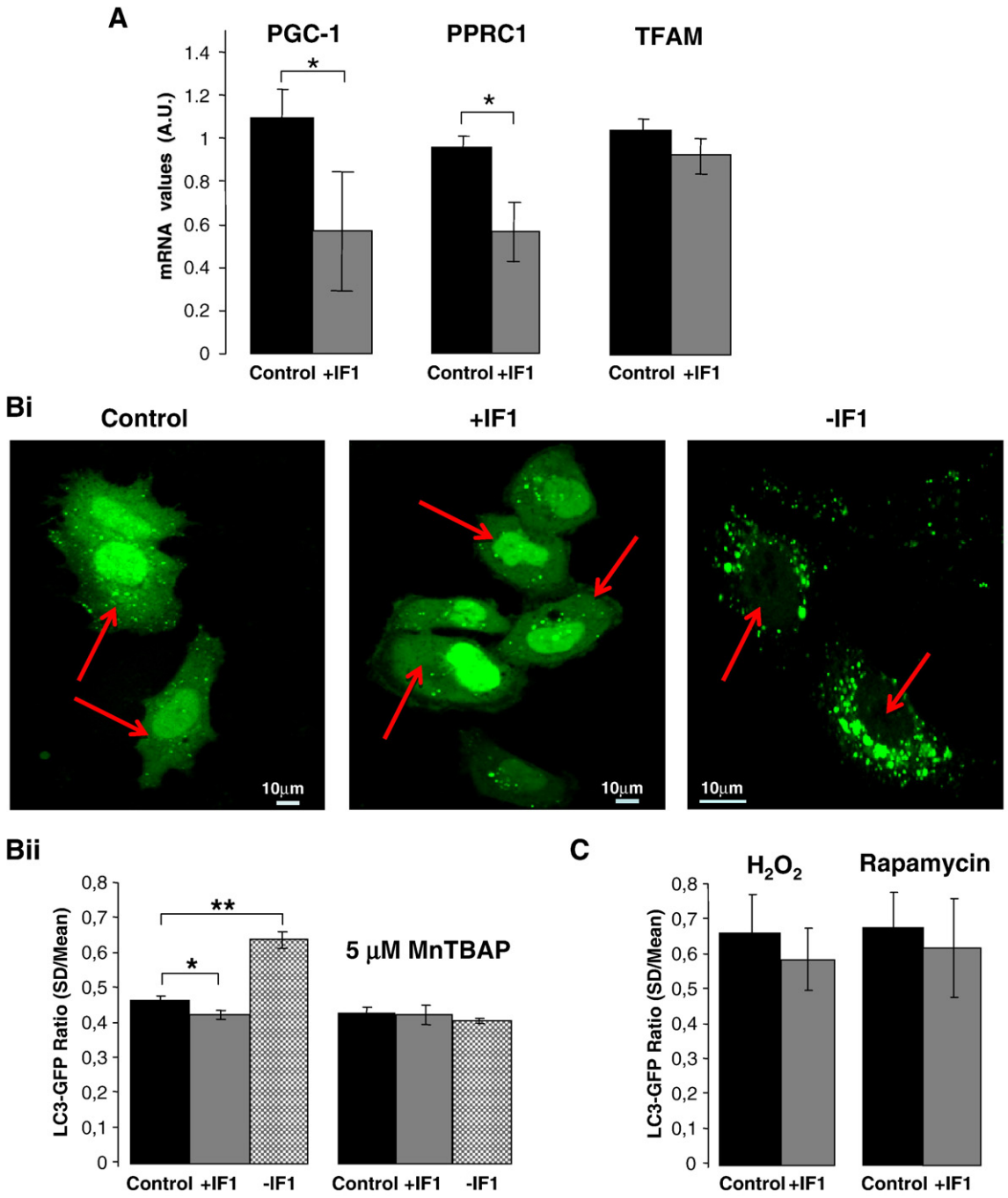

Fig. 2. Autophagosome formation is depending on IF1 level of expression just at resting conditions and is avoided by treatment with ROS scavenger. (A) rtPCR analysis of mRNA levels of the mitochondrial biogenesis regulators PGC1, PPRC1and TFAM did not show any rise in expression in +IF1 cells and even suggested a statistically significant reduction for PGC1 and PPRC1. Bi shows representative confocal images of LC3-GFP distribution in HeLa cells expressing different levels of IF1. Following activation of autophagy, LC3-GFP accumulates at autophagosomal membranes and serves as a specific marker of the process. At resting conditions, the number of green puncta (autophagosomes) present in the cytosol of $-IF_1$ cells was significantly greater than in control and $+IF_1$ cells. This was quantified by calculating the standard deviation/mean ratio of pixel intensity in the LC3-GFP positive cells as shown in panel Bii. SD/mean ratio was increased in −IF1 cells, indicating a greater level of basal autophagic activity than in control and +IF1 cells. 12 h treatment with 5 μM MnTBAP, a ROS scavenger, normalized the differences in the SD/mean ratios in $+IF_1$ and $-IF_1$ cells, which show similar % of LC3-GFP translocation to the autophagosomes. Panel C reports that overexpression of IF1 had no effect against autophagosome formation triggered by H_2O_2 (10^{-6}M, 2 h) or Rapamycin (5 μM, 4 h), confirming that changes in autophagy with IF1 expression level are responses to differences in intrinsic mitochondrial ROS generation.

MnTBAP might also prevent the changes in mitochondrial volume recorded at 36 h after IF1 suppression. Therefore, 24 after transfection, cells co-transfected with IF1siRNA (−IF1 cells) and mitochondrially targeted EGFP were treated with 5 μM MnTBAP for 12 h (the same protocol employed before). The data presented in Fig. 3B show that the mitochondrial mass was preserved in −IF1 cells treated with MnTBAP. Quantification of the mitochondrial volume occupancy presented in Fig. 3Ci performed as above, revealed a rise in the volume area occupied by mitochondria in MnTBAP treated cells, quantified in panel 3Cii (−IF1:22.6%±6.3; −IF1+MnTBAP: 46.3%±12.8, $*p<0.05$; $n=3$ sets of transfection). However, the mitochondrial network still appeared disorganized; suggesting that IF1 suppression still alters mitochondrial morphology although the overall volume was preserved in the presence of MnTBAP.

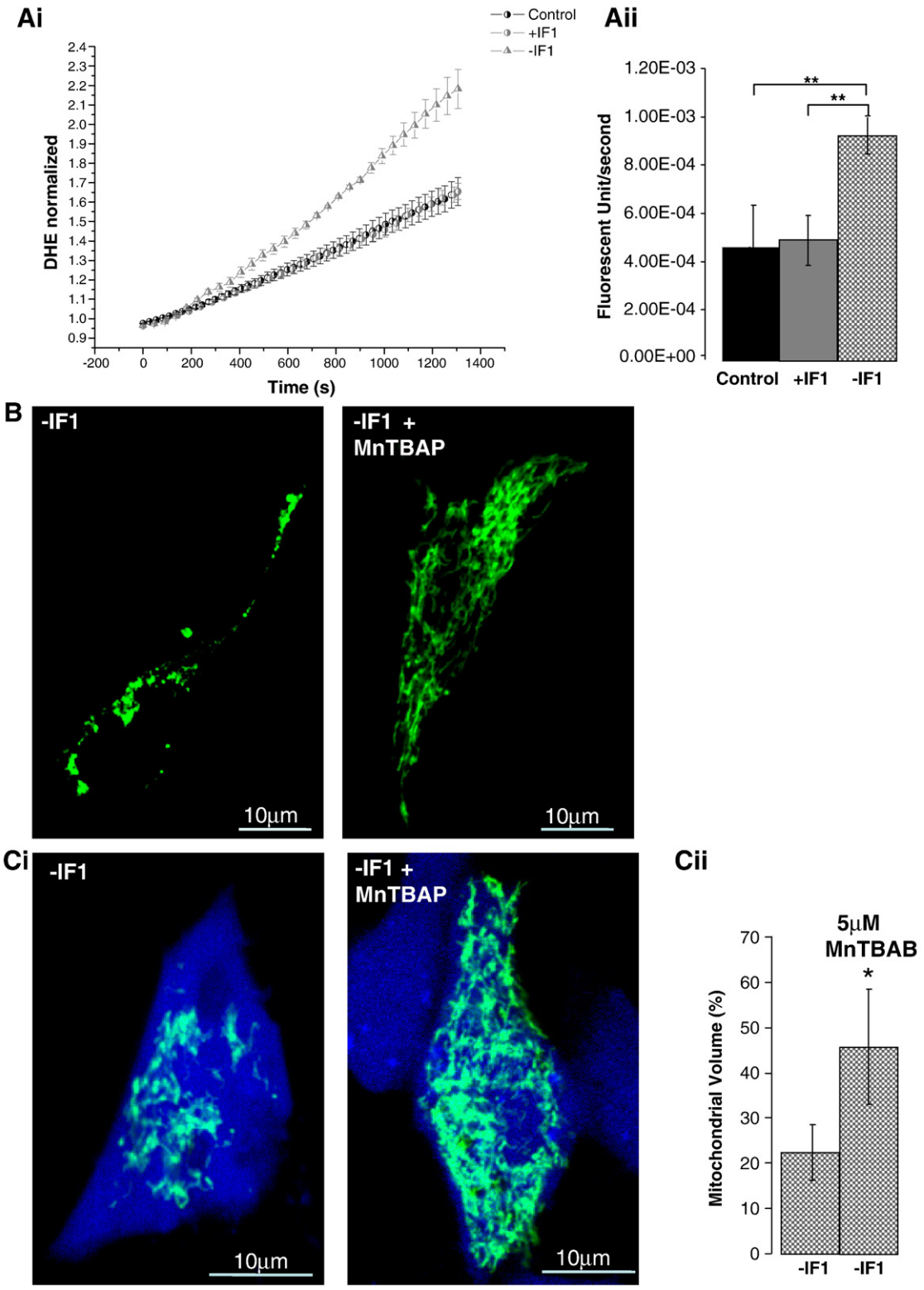

Fig. 3. The rate of generation of reactive oxygen species (ROS) is increased in −IF1 cells and treatment with a ROS scavenger preserved the mitochondrial network. The rate of intracellular ROS generation in HeLa cells with altered expression of IF1 was measured using dihydroethidium (DHE, 10 μM). Traces reported in panel Ai indicate that rates of ROS production between control and −IF1 cells were statistically different. Values obtained are summarized and plotted in panel Aii. B shows confocal images of −IF1 HeLa cells 36 h after transfection untreated (let hand panel) or treated 12 h with MnTBAP. The ROS scavenger helped to preserve the mitochondrial network. The cell volume occupied by mitochondria in −IF1 cells with and without MnTBAB was measured as described above using calcein blue (Ci) and shown in Cii.

2.5. Co-visualization of autophagosome formation and mitochondrial network morphology

In order to combine the results obtained on mitochondrial volume and autophagy activity, we co-transfected cells with a mitochondrially targeted red fluorescent protein (mt-RFP) and the LC3-GFP fusion protein in HeLa cells expressing different levels of IF1. Representative images show that increased mitochondrial volume (mt-RFP) corresponds to a diffuse cytosolic distribution of LC3-GFP (Fig. 4). Conversely, when the mitochondrial network was disrupted in −IF1 cells, LC3-GFP showed a more punctuate pattern implying a higher level of autophagosome activity. We have also calculated and plotted

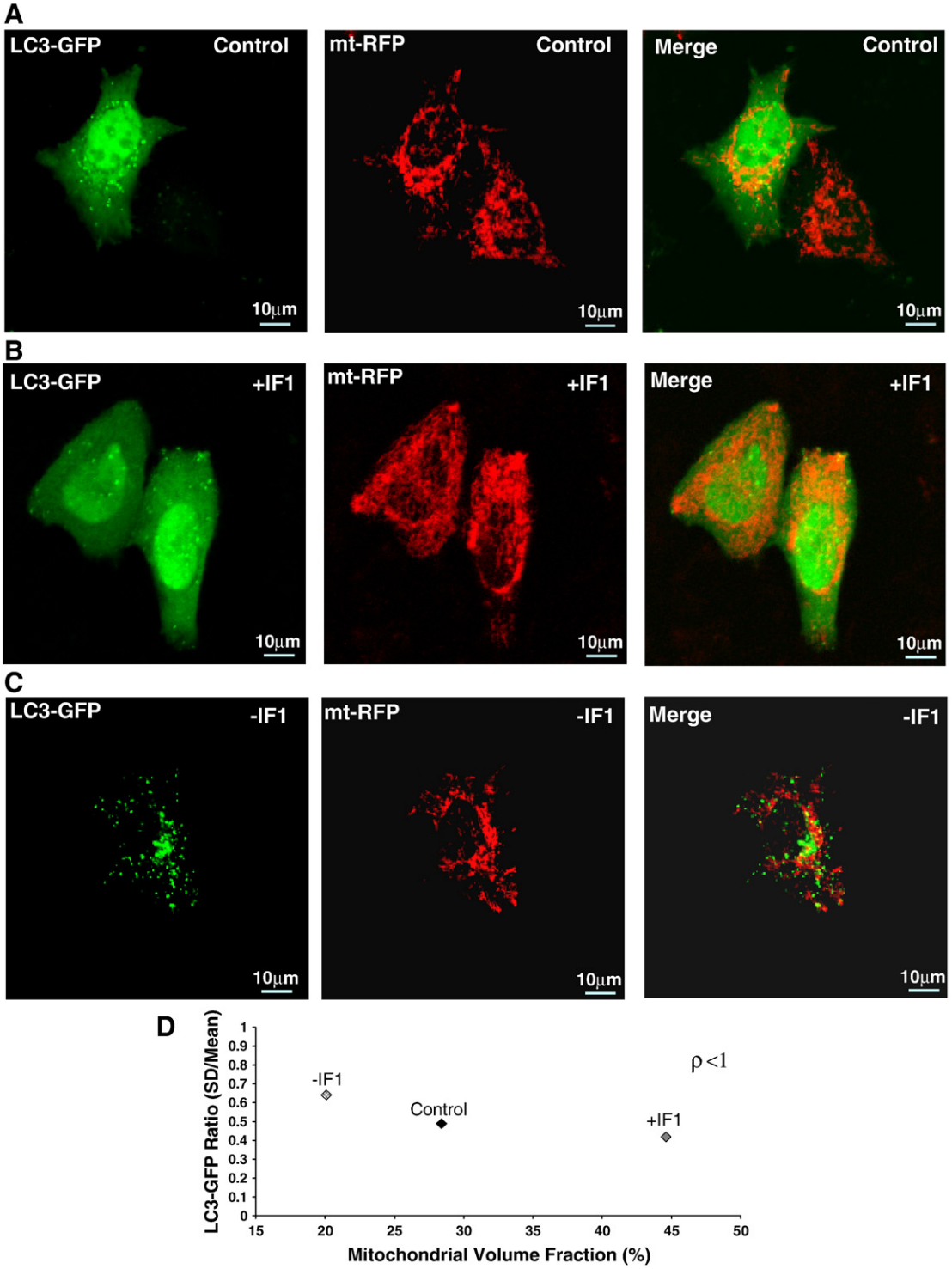

Fig. 4. Mitochondrial volume reduction coincides with increased level of autophagy. Representative confocal images of HeLa cells expressing altered levels of IF1 and co-transfected with mitochondrially targeted red variant of GFP to visualize mitochondrial structure and LC3-GFP to monitor the level of autophagy are shown in panel A, B and C. Cytosolic localization of LC3-GFP coincided with preservation of the mitochondrial network in +IF1 cells whilst localization of LC3-GFP to autophagosomes correlated with a decreased mitochondrial volume fraction in −IF1 cells ($n=4$ per type of transfection). A plot generated from the comparison of the pairs of values is represented in panel D highlighting the inverted relation between autophagy and mitochondrial volume.

(Fig. 4 Panel D) the correlation coefficient between the two variables: LC3-GFP ratio and mitochondrial volume fraction. This disclosed an inverse relationship between autophagic activity and mitochondrial volume ($\rho = 0.863$).

3. Discussion

We have found that mitochondrial volume in HeLa cells varies according to the level of IF1 expression. Thus, in IF1 overexpressing cells, the fraction of the cell volume occupied by mitochondria was significantly increased compared to controls. Conversely, suppression of IF1 promoted the opposite result with a decrease in mitochondrial volume fraction (Fig. 1). Therefore, in IF1 overexpressing cells, the expression level of genes responsible for mitochondrial biogenesis was investigated and by rtPCR the RNA messenger level of PGC1-α, PPRC and TFAM quantified (Fig. 2A). Since none of these increased, (in the case of PGC1-α and PPRC there was even a significant reduction), we wondered whether the changes in mitochondrial volume might reflect rather alterations in catabolic processes such as autophagy. Autophagy is the only self conservatory mechanism in nucleated cells, compatible with cell survival, able to remove organelles from the cytoplasm. In recent years, an increased understanding of the role of autophagy in the control of mitochondrial degradation has been developed [31,32]. Autophagy is typically activated by fasting and nutrient deprivation and also removes toxic protein aggregates and unneeded organelles, whilst insufficient or deregulated autophagy can promote cell injury [33].

LC3 migrates from its cytosolic localization during autophagy to newly formed autophagosomes marking the degree of autophagy activation and representing so an ideal tool to monitor this process. Using the autophagosome marker, LC3-GFP, we found that IF1 overexpression reduced autophagosomal activity whilst −IF1 cells showed obvious punctuate LC3-GFP distribution, suggesting increased autophagosomal activity (Fig. 2B). Thus, autophagy seems to be the major process underlying the changes in mitochondrial volume fraction that we have seen associated with manipulations of IF1 expression.

Since mammals – unlike yeast [34] – apparently lack proteins acting as specific molecules that tag mitochondria to be removed, the signalling might well be derived from mitochondrial metabolism. The production of reactive oxygen species (ROS) may represent an obvious signalling pathway to regulate autophagic removal of mitochondria — mitophagy [35–38]. Thus, oxidative stress induced using H_2O_2 or 2-methoxyestradiol (2-ME) induces autophagy in HeLa cells [39]. Furthermore, the use of ROS scavengers or the overexpression of superoxide dismutase significantly reduced the levels of autophagy in HeLa cells [40]. Mitochondrial ROS generation depends on mitochondrial metabolism (for review see [41]) and may constitute the mechanism by which damaged mitochondria are selectively targeted by autophagy. We found here that the ROS scavenger MnTBAP, a superoxide dismutase mimetic, prevented the increased autophagy seen in the −IF1 cells (Fig. 2Bii), suggesting that IF1 knock down increased ROS production, which was confirmed using Dihydroethidium (DHE). We have shown recently that IF1 suppression is associated with a more reduced level of the NADH:NAD+ ratio and an increase in $\Delta\psi_m$ which we have attributed to a decreased proton flux through the ATP synthase [7]. These conditions favour mitochondrial ROS generation [42,43] associated with increased $\Delta\psi_m$ values [44]. Therefore, IF1 downregulation renders mitochondria less “bio-energetically competent” promoting an increased rate of ROS production. This in turn drives selective mitochondrial degradation by autophagy and induces scaling down of the mitochondrial network.

As further confirmation of the ROS dependence of this process, MnTBAP efficiently counteracts this phenomenon in −IF1 cells (Fig. 3Bi and Bii). It is important to note that autophagy induced by exogenous oxidative stress was not influenced by IF1 expression, nor was that induced with the immunosuppressant Rapamycin. Thus, the autophagy seen in the −IF1 cells is a response to altered intrinsic signalling pathways, and is not a secondary response to other downstream components of the pathway that might be influenced by subtle changes in cellular bioenergetics promoted by IF1 expression level.

Simultaneous imaging of autophagosome formation and the appearance of the mitochondrial network (see Fig. 4) established the negative correlation between these two variables and its dependence on IF1 expression level. These data suggest that IF1 is a housekeeping gene in mitochondrial quality control since its deletion increases autophagy and decreases the mitochondrial volume fraction. Therefore, malfunctioning mitochondria such as those without IF1 produce un-physiological levels of ROS that make them targeted by autophagy thus affecting the overall mitochondrial volume.

However, we cannot rule out the morphological modifications occurring at ultrastructural level and attributed to IF1 as co-mediators in the mitochondrial turnover. Indeed, recent reports indicate that mitophagy requires a dismantling of the inner mitochondrial structure through disruption of cristae junctions. For example, the level of Optic Atrophy type 1 (OPA1) [45], is downregulated before mitophagy [46]. This implies that a tuned combination of events occurring at retrograde (structural modifications) and post mitochondrial level (ROS generation) may be needed for the execution of mitophagy. It therefore seems that IF1 plays an unexpected role in this process due to its capacity to impinge on both levels of mitochondrial regulation: structure and function.

Although these findings fit with the conceptual background set out in our previous studies [7], the role for IF1 in normal respiring mitochondria is controversial. In bovine heart submitochondrial vesicles, an increase in IF1 expression was associated with inhibition of F_1F_o-ATPsynthase activity [47,48]. Very recently, reduction of mitochondrial F_1F_o-ATPsynthase/ATPase activity was associated with the silencing of the immediate early gene *IEX-1*, a gene that targets and degrades IF1 [49]. However, a clear understanding of the protein's role in physiological conditions is hard to elucidate until the nature of the interaction between IF1 and the F_1F_o-ATPsynthase in respiring mitochondria is fully characterized.

We found, via blue native gel analysis, that in HeLa cells overexpressing IF1 the ratio of dimeric to monomeric forms of the F_1F_o protein complex was increased [7], consistent with findings in hepatoma cells [50]. This finding also remains controversial. Thus, according to Zanotti et al. [51] the high affinity binding of IF1 for the F_1F_o-ATPsynthase would prevent the formation of any dimer whilst more recently it has been proposed that IF1 mediated dimerization would help stabilize the inhibitory complex with the F_1F_o-ATPase [52].

Our vision for IF1 as coupling factor lacks direct biochemical evidence and so must be considered as speculative, however our data are internally consistent and supported by studies of rat neurons in culture and kidney slices which showed that the IF1:F_1F_o-ATP synthase ratios are high in oxidative cell types (neurons and proximal tubules) and low in their more glycolytic neighbouring cells, the astrocytes and distal renal tubules respectively [7,53].

The data presented in the current report suggest that, by affecting basal cellular autophagy, IF1 may play an unexpected role in mitochondrial quality control. These observations broaden the apparent roles of this molecule that seems to play an important and complex role in the regulation of cellular and mitochondrial homeostasis.

4. Materials and methods

4.1. Reagents

Rapamycin, Hydrogen peroxide (H_2O_2) were purchased from SIGMA-Aldrich, manganese (III) tetrakis (4-benzoic acid) porphyrin (MnTBAB) from Calbiochem.

4.2. Cell culturing and transfection

All the experiments of this study were carried out using the HeLa cell line (Human Cervical Adenocarcinoma cells). HeLa cells were grown in a DMEM culture medium, made up of DMEM (Gibco™ 41966), supplemented with 10% Fetal Bovine Serum (FBS-Gibco™ 10106-185), 50 U/ml Penicillin and 25 μg/ml Streptomycin. In all experiments, the transfection of DNA was carried out using Lipofectamine Reagent (Invitrogen™ 18324-012), according to the manufactures' protocol. As previously described [7] in order to over-express IF1 in HeLa cells, the cells were transfected with IF1-cDNA (Open Biosystems, Invitrogen™ MHS1010-73732), whereas small interfering RNA (siRNA) (Qiagen S100908075) was used to suppress the expression of IF1. Mitochondrial morphology was imaged using Green Fluorescent Protein Targeted to mitochondria (mtGFP). For the imaging experiments together with the LC3-GFP, mitochondria were instead imaged with the red variant of the GFP targeted to mitochondria through a kinase anchoring protein (AKAP).

4.3. Investigating mitochondrial morphology

HeLa cells expressing mtGFP and altered levels of IF1 were washed with phosphate buffered saline (PBS), were place into a saline which we shall refer to as Recording Medium (RM) consisting of (mM): NaCl 156; KCl 3: $MgSO_4$ 2; KH_2PO_4 125; D-Glucose 10; $CaCl_2$ 2; Hepes (Gibco™ 15630-056) 10; with pH 7.3–7.4. 2.5 μL calcein blue (Invitrogen™ 23338) was then added to the RM and then mixed and allowed to load for 5 min at room temperature.

Images were acquired using a Zeiss 510 CLSM confocal microscope with a Plan-Apochromat ×63/1.4 oil immersion objective lens at RT. Calcein blue was excited with a 364 nm wavelength laser and mtGFP with a 488 nm laser. Laser power was kept as low as possible (0.1–2%), to avoid bleaching of the signal.

Images were analyzed using the software program Image J. The two channels (calcein blue and mtGFP) were separated and thresholded in order to acquire two separate binary images. The proportion of the cytoplasm (stained with calcein blue) occupied by the mitochondrial network was then calculated from the area of both images (represented by mtGFP image). The process is illustrated in Supplementary Fig. 1B. In order to control for observer bias, the identity of the transfected cells was blinded and analysis was carried out twice, with an average for each cell taken.

4.4. Measuring the levels of autophagy

LC3-GFP was used as a marker for autophagy. During the activation of autophagy, the cytosolic form of the microtubule-associated protein light chain 3 LC3 (LC3-I) is cleaved and conjugated with phosphatidylethanolamine (PE), resulting in the formation of LC3-II [54]. This form then translocates from the cytosol to the newly formed autophagosomal membrane. Therefore, the fusion of LC3 with green fluorescent protein, allows it to serve as a specific indicator of autophagosomes [55], appearing as punctuate by fluorescence microscopy [56]. HeLa cells were transfected with LC3-GFP using lipofectamine. 36 h after transfection, the cells (growing on cover slips) were mounted in a microscope chamber, washed with RM, and imaged using a Zeiss 510 CLSM. The images were analyzed using the Zeiss 510 Software. The mean signal and standard deviation of the mean of pixel intensity within individual cells was measured. Cells with increased levels of autophagic activity were identified as those containing a greater number of autophagosomes, which was quantified as an increase in SD as there is a greater variability in pixel intensity in these cells (between the bright autophagosomes and the dark cytosol). However, in control cells, the LC3-GFP was uniformly distributed throughout the cytosol, (i.e. SD was low). Moreover, in order to correct for differences in overall brightness between different images, since the expression of LC3-GFP was not the same in all cells, the standard deviation was divided by the mean pixel intensity within the area of the image analyzed. To measure the levels of autophagy following treatment with MnTBAP, twenty-four(24) hours following transfection with LC3-GFP, HeLa cells were treated with 5 μM of manganese (III) tetrakis (4-benzoic acid) porphyrin (MnTBAP), a cell-permeable superoxide dismutase mimetic [57]. The cells were incubated with MnTBAP for 12 h and were then washed once with sterile PBS. The cover slips were then mounted in chambers and loaded with RM. Cell imaging and data analysis were carried out as described above.

4.5. Quantitative real time RT-PCR

Total RNA was obtained using the Rneasy Plus Minikit (Qiagen) and 1.5 μg of RNA reverse transcribed with Superscript II Reverse Transcriptase (Invitrogen). Quantitative PCR was performed using the Dynamo™ SYBR® Green qPCR Kit (Finnzymes) and the Opticon 2 DNA engine (MJ Research). Gene-specific primer pairs for PGC1α (Forward:cctgcatgagtgtgtgctct;Reverse:gcaaagaggctggtcttcac), PPRC1 (Forward:ctggccctcctgaaaatgta; Reverse:caggctcctcaacagtcaca).

And TFAM (Forward:gggttccagttgtgattgct; Reverse: tggacaacttgccaagacag) were designed using the Primer3 algorithm [58].

4.6. Measurements of ROS production

Coverslips were transferred to small chambers for microscopy. Cells were imaged whilst bathed in RM. Dihydroethidium (DHE; 10 μM) was added immediately before the start of an experiment and remained in the solution for the duration. Images were obtained using a Zeiss 510 LSM confocal microscope using a 40× oil immersion lens. Excitation was provided by the 543 line of the helium–neon laser line and emitted fluorescence collected >560 nm. In all experiments using DHE, data were collected every 10 s. The rate of DHE oxidation in cells transfected with the empty vector was compared with the rate of DHE oxidation in +IF1 or −IF1. The rate was calculated in every cell in a field of view was analyzed and included in the final measurements.

4.7. Statistics

The probability of statistically significant differences between two experimental groups was determined by Student's *T* test. Values are expressed as mean ± SDV of at least three independent experiments unless stated otherwise.

Acknowledgements

We thank Prof. Rosario Rizzuto for mtGFP construct, Dr. Gyorgy Szabadkai for LC3-GFP and mt-RFP constructs and critical reading of the paper, Mr Gianluca Verlengia for help in collecting the ROS data. We would like also to acknowledge Marie Curie Actions for supporting MC as IntraEuropean Fellow at the time of the experiments. We thank the Wellcome Trust for supporting AS through a summer studentship and for grant support to MRD, and the RVC internal funds granted to MC.

Appendix A. Supplementary data

Supplementary data associated with this article can be found, in the online version, at doi:10.1016/j.bbabio.2009.02.023.

References

[1] J.P. Abrahams, A.G. Leslie, R. Lutter, J.E. Walker, Structure at 2.8 A resolution of F1-ATPase from bovine heart mitochondria, Nature 370 (1994) 621.
[2] P.D. Boyer, The ATP synthase—a splendid molecular machine, Annu. Rev. Biochem. 66 (1997) 717.

[3] J.E. Walker, A.L. Cozens, M.R. Dyer, I.M. Fearnley, S.J. Powell, M.J. Runswick, Structure and genes of ATP synthase, Biochem. Soc. Trans. 15 (1987) 104.
[4] J. Moyle, P. Mitchell, Proton translocation quotient for the adenosine triphosphatase of rat liver mitochondria, FEBS Lett. 30 (1973) 317.
[5] Y. Hatefi, The mitochondrial electron transport and oxidative phosphorylation system, Annu. Rev. Biochem. 54 (1985) 1015.
[6] D.W. Green, G.J. Grover, The IF(1) inhibitor protein of the mitochondrial F(1)F(0)-ATPase, Biochim. Biophys. Acta 1458 (2000) 343.
[7] M. Campanella, E. Casswell, S. Chong, Z. Farah, M.R. Wieckowski, A.Y. Abramov, A. Tinker, M.R. Duchen, Regulation of mitochondrial structure and function by the F1Fo-ATPase inhibitor protein, IF1, Cell Metab. 8 (2008) 13.
[8] B. Levine, D.J. Klionsky, Development by self-digestion: molecular mechanisms and biological functions of autophagy, Dev. Cell 6 (2004) 463.
[9] F. Reggiori, T. Shintani, U. Nair, D.J. Klionsky, Atg9 cycles between mitochondria and the pre-autophagosomal structure in yeasts, Autophagy 1 (2005) 101.
[10] F. Reggiori, 1. Membrane origin for autophagy, Curr. Top. Dev. Biol. 74 (2006) 1.
[11] P.O. Seglen, T.O. Berg, H. Blankson, M. Fengsrud, I. Holen, P.E. Stromhaug, Structural aspects of autophagy, Adv. Exp. Med. Biol. 389 (1996) 103.
[12] K. Suzuki, T. Kirisako, Y. Kamada, N. Mizushima, T. Noda, Y. Ohsumi, The pre-autophagosomal structure organized by concerted functions of APG genes is essential for autophagosome formation, EMBO J. 20 (2001) 5971.
[13] Y. Ohsumi, N. Mizushima, Two ubiquitin-like conjugation systems essential for autophagy, Semin. Cell Dev. Biol. 15 (2004) 231.
[14] Z. Xie, D.J. Klionsky, Autophagosome formation: core machinery and adaptations, Nat. Cell Biol. 9 (2007) 1102.
[15] T.P. Neufeld, Genetic analysis of TOR signaling in Drosophila, Curr. Top. Microbiol. Immunol. 279 (2004) 139.
[16] S. Pattingre, A. Tassa, X. Qu, R. Garuti, X.H. Liang, N. Mizushima, M. Packer, M.D. Schneider, B. Levine, Bcl-2 antiapoptotic proteins inhibit Beclin 1-dependent autophagy, Cell 122 (2005) 927.
[17] J.C. Farre, S. Subramani, Peroxisome turnover by micropexophagy: an autophagy-related process, Trends Cell Biol. 14 (2004) 515.
[18] B.M. Spiegelman, Transcriptional control of energy homeostasis through the PGC1 coactivators, Novartis. Found. Symp. 286 (2007) 3.
[19] C. Handschin, B.M. Spiegelman, Peroxisome proliferator-activated receptor gamma coactivator 1 coactivators, energy homeostasis, and metabolism, Endocr. Rev. 27 (2006) 728.
[20] D. Kang, S.H. Kim, N. Hamasaki, Mitochondrial transcription factor A (TFAM): roles in maintenance of mtDNA and cellular functions, Mitochondrion. 7 (2007) 39.
[21] P. Golstein, G. Kroemer, A multiplicity of cell death pathways. Symposium on apoptotic and non-apoptotic cell death pathways, EMBO Rep. 8 (2007) 829.
[22] R. Scherz-Shouval, Z. Elazar, ROS, mitochondria and the regulation of autophagy, Trends Cell Biol. 17 (2007) 422.
[23] R. Scherz-Shouval, E. Shvets, Z. Elazar, Oxidation as a post-translational modification that regulates autophagy, Autophagy 3 (2007) 371.
[24] R. Scherz-Shouval, E. Shvets, E. Fass, H. Shorer, L. Gil, Z. Elazar, Reactive oxygen species are essential for autophagy and specifically regulate the activity of Atg4, EMBO J. 26 (2007) 1749.
[25] B.J. Day, S. Shawen, S.I. Liochev, J.D. Crapo, A metalloporphyrin superoxide dismutase mimetic protects against paraquat-induced endothelial cell injury, in vitro, J. Pharmacol. Exp. Ther. 275 (1995) 1227.
[26] V.P. Bindokas, J. Jordan, C.C. Lee, R.J. Miller, Superoxide production in rat hippocampal neurons: selective imaging with hydroethidine, J. Neurosci. 16 (1996) 1324.
[27] T. Zhao, V. Benard, B.P. Bohl, G.M. Bokoch, The molecular basis for adhesion-mediated suppression of reactive oxygen species generation by human neutrophils, J. Clin. Invest. 112 (2003) 1732.
[28] A.Y. Abramov, J. Jacobson, F. Wientjes, J. Hothersall, L. Canevari, M.R. Duchen, Expression and modulation of an NADPH oxidase in mammalian astrocytes, J. Neurosci. 25 (2005) 9176.
[29] H. Zhao, S. Kalivendi, H. Zhang, J. Joseph, K. Nithipatikom, J. Vasquez-Vivar, B. Kalyanaraman, Superoxide reacts with hydroethidine but forms a fluorescent product that is distinctly different from ethidium: potential implications in intracellular fluorescence detection of superoxide, Free Radic. Biol. Med. 34 (2003) 1359.
[30] V.P. Bindokas, J. Jordan, C.C. Lee, R.J. Miller, Superoxide production in rat hippocampal neurons: selective imaging with hydroethidine, J. Neurosci. 16 (1996) 1324.
[31] S. Rodriguez-Enriquez, I. Kim, R.T. Currin, J.J. Lemasters, Tracker dyes to probe mitochondrial autophagy (mitophagy) in rat hepatocytes, Autophagy 2 (2006) 39.
[32] D. Mijaljica, M. Prescott, D.J. Klionsky, R.J. Devenish, Autophagy and vacuole homeostasis: a case for self-degradation? Autophagy 3 (2007) 417.
[33] B. Levine, G. Kroemer, Autophagy in the pathogenesis of disease, Cell 132 (2008) 27.
[34] T. Kanki, D.J. Klionsky, Mitophagy in yeast occurs through a selective mechanism, J. Biol. Chem. 283 (2008) 32386.
[35] Y. Chen, E. Millan-Ward, J. Kong, S.J. Israels, S.B. Gibson, Mitochondrial electron-transport-chain inhibitors of complexes I and II induce autophagic cell death mediated by reactive oxygen species, J. Cell Sci. 120 (2007) 4155.
[36] Y. Chen, E. Millan-Ward, J. Kong, S.J. Israels, S.B. Gibson, Oxidative stress induces autophagic cell death independent of apoptosis in transformed and cancer cells, Cell Death Differ. 15 (2008) 171.
[37] R. Scherz-Shouval, Z. Elazar, ROS, mitochondria and the regulation of autophagy, Trends Cell Biol. 17 (2007) 422.
[38] R. Scherz-Shouval, E. Shvets, E. Fass, H. Shorer, L. Gil, Z. Elazar, Reactive oxygen species are essential for autophagy and specifically regulate the activity of Atg4, EMBO J. 26 (2007) 1749.
[39] Y. Chen, E. Millan-Ward, J. Kong, S.J. Israels, S.B. Gibson, Oxidative stress induces autophagic cell death independent of apoptosis in transformed and cancer cells, Cell Death. Differ. 15 (2008) 171.
[40] Y. Chen, E. Millan-Ward, J. Kong, S.J. Israels, S.B. Gibson, Oxidative stress induces autophagic cell death independent of apoptosis in transformed and cancer cells, Cell Death. Differ. 15 (2008) 171.
[41] M.P. Murphy, How mitochondria produce reactive oxygen species, Biochem. J. 417 (2009) 1.
[42] V. dam-Vizi, C. Chinopoulos, Bioenergetics and the formation of mitochondrial reactive oxygen species, Trends Pharmacol. Sci. 27 (2006) 639.
[43] M.P. Murphy, How mitochondria produce reactive oxygen species, Biochem. J. 417 (2009) 1.
[44] S.S. Korshunov, V.P. Skulachev, A.A. Starkov, High protonic potential actuates a mechanism of production of reactive oxygen species in mitochondria, FEBS Lett. 416 (1997) 15.
[45] C. Frezza, S. Cipolat, B.O. Martins de, M. Micaroni, G.V. Beznoussenko, T. Rudka, D. Bartoli, R.S. Polishuck, N.N. Danial, S.B. De, L. Scorrano, OPA1 controls apoptotic cristae remodeling independently from mitochondrial fusion, Cell 126 (2006) 177.
[46] G. Twig, A. Elorza, A.J. Molina, H. Mohamed, J.D. Wikstrom, G. Walzer, L. Stiles, S.E. Haigh, S. Katz, G. Las, J. Alroy, M. Wu, B.F. Py, J. Yuan, J.T. Deeney, B.E. Corkey, O.S. Shirihai, Fission and selective fusion govern mitochondrial segregation and elimination by autophagy, EMBO J. 27 (2008) 433.
[47] I. Husain, D.A. Harris, ATP synthesis and hydrolysis in submitochondrial particles subjected to an acid-base transition. Effects of the ATPase inhibitor protein, FEBS Lett. 160 (1983) 110.
[48] G. Lippe, M.C. Sorgato, D.A. Harris, Kinetics of the release of the mitochondrial inhibitor protein. Correlation with synthesis and hydrolysis of ATP, Biochim. Biophys. Acta 933 (1988) 1.
[49] L. Shen, L. Zhi, W. Hu, M.X. Wu, IEX-1 targets mitochondrial F1Fo-ATPase inhibitor for degradation, Cell Death Differ. (2008).
[50] J.J. Garcia, E. Morales-Rios, P. Cortes-Hernandez, J.S. Rodriguez-Zavala, The inhibitor protein (IF1) promotes dimerization of the mitochondrial F1F0-ATP synthase, Biochemistry 45 (2006) 12695.
[51] F. Zanotti, G. Raho, A. Gaballo, S. Papa, Inhibitory and anchoring domains in the ATPase inhibitor protein IF1 of bovine heart mitochondrial ATP synthase, J. Bioenerg. Biomembr. 36 (2004) 447.
[52] N. Buzhynskyy, P. Sens, V. Prima, J.N. Sturgis, S. Scheuring, Rows of ATP synthase dimers in native mitochondrial inner membranes, Biophys. J. (2007).
[53] A.M. Hall, R. Unwin, N. Parker, M.R. Duchen, Multi-photon imaging reveals differences in mitochondrial function between nephron segments, J. Am. Soc. Nephrol. (2009).
[54] Y. Kabeya, N. Mizushima, T. Ueno, A. Yamamoto, T. Kirisako, T. Noda, E. Kominami, Y. Ohsumi, T. Yoshimori, LC3, a mammalian homologue of yeast Apg8p, is localized in autophagosome membranes after processing, EMBO J. 19 (2000) 5720.
[55] Y. Kabeya, N. Mizushima, A. Yamamoto, S. Oshitani-Okamoto, Y. Ohsumi, T. Yoshimori, LC3, GABARAP and GATE16 localize to autophagosomal membrane depending on form-II formation, J. Cell Sci. 117 (2004) 2805.
[56] N.R. Brady, A. Hamacher-Brady, H. Yuan, R.A. Gottlieb, The autophagic response to nutrient deprivation in the hl-1 cardiac myocyte is modulated by Bcl-2 and sarco/endoplasmic reticulum calcium stores, FEBS J. 274 (2007) 3184.
[57] B.J. Day, S. Shawen, S.I. Liochev, J.D. Crapo, A metalloporphyrin superoxide dismutase mimetic protects against paraquat-induced endothelial cell injury, in vitro, J. Pharmacol. Exp. Ther. 275 (1995) 1227.
[58] S. Rozen, H. Skaletsky, Primer3 on the WWW for general users and for biologist programmers, Methods Mol. Biol. 132 (2000) 365.